**SIMULATIONS OF THE INFLUENCE OF THE GRAINS ORIENTATIONS ON ULTRASOUNDS**

A. Apfel[1], J. Moysan[1], G. Corneloup[1], B. Chassignole [2]
[1] Laboratoire de Caractérisation Non Destructive (LCND, EA 3153), Université de la Méditerranée, France, [2] Electricité de France, Recherche et Développement, Les Renardières, France

**Abstract:** In some austenitic stainless steel welds grains orientations cause deviation and splitting of the ultrasonic beam. It is especially true in the case of multipass welds when the remelting process after each pass causes complex solidification process. With the new model MINA (Modelling anisotropy from Notebook of Arc welding) we show that we are able to predict thoroughly grains orientations. This model has been validated with microstructural analysis and ultrasonic measurements. With these orientations we define a precise description of the heterogeneous and anisotropic material. Grain orientation give the Cartesian coordinates system in which we expressed the elastic constants. Incorporating this description in an ultrasonic propagation code allows simulating ultrasonic inspection. Comparisons are made with previous models given by several authors. The reference grain structure is obtained by macrograph analysis. Different propagations of the elastic waves induced by a modification of the evolution of the grains orientations are shown. The best simulation results are obtained with MINA model. We thus provide a very interesting model dedicated to multipass welding to improve understanding of ultrasounds propagation in a very heterogeneous medium. This work ensures a better reliability of ultrasonic testing.

**Introduction:** The ultrasonic assessment of structural integrity in nuclear power station progresses with advances in ultrasonic wave propagation codes. It makes ultrasonic testing more accurate and reliable. Several modelling codes have been proposed to forecast the propagation of ultrasounds. Authors use ray tracing codes, semi-analytical codes or finite element codes. Developments concerned three steps: a calculation of ultrasonic fields radiated by transducers, a calculation of the ultrasonic wave propagation and a simulation of the various echo-formation mechanisms. Descriptions and comparisons of these modelling techniques are found in literature [1-3]. An efficient simulation depends on an accurate description of the material properties. It is well known that inspection of components composed of austenitic steel can cause difficulties. Several large demonstrating programmes highlighted this phenomenon: the projects PISC (**P**rogramme for the **I**nspection of **S**teel **C**omponents) [4-5] or the **D**efect **D**etection **T**rial [4]. Theses major international efforts were made to improve the assessment of capability and reliability of procedures for non-destructive testing. Best results were obtained in the case of ferritic steels with easy access. Performances decreased when access difficulties increased. Lowest results were obtained with cast austenitic steel welds [6-8]. It was concluded that there is a growing need for precise description of the weld material to improve the capability of simulating real weld testing.

The source of the difficulties lies in the grains structure of austenitic steels. The ultrasonic wave equation could be written in the form:

$$\rho \frac{\partial^2 u_i}{\partial t^2} = C_{ijkl} \frac{\partial^2 u_k}{\partial x_j \partial x_l} \qquad (1)$$

where $\underline{u}$ is the particle displacement, $\rho$ is the density and the $C_{ijkl}$ are the appropriate elastic constants. The solution of this equation leads to the well-known Christoffel equation [9]:

$$\rho V^2 \delta_{i\lambda} - C_{ijk\lambda} n_j n_k = 0 \qquad (2)$$

where $\delta_{il}$ is the Kronecker symbol; V the phase velocity, $\underline{n}$ is the propagation direction (for details see reference [9]). In general three solutions are obtained for a given wave propagation direction. Equation (2) shows that a strong dependence exists between the wavevector direction $\underline{n}$ and the wave velocity.

An austenitic grain is most often considered as an orthotropic material but it is possible to use a transversely isotropic system to describe the grain material [10]. In the literature, tensor value of the elastic constants showed significant variations of values according to the steel composition. Measurements made by X-diffractometry and by ultrasound enabled to determine the elastic constants. The ultrasonic method uses speed measurements at different angles of incidences on metal sheets cut in the weld. This method is now sufficiently well known to determine the elastic constants with good accuracy. [11-12].

Elastic constants correspond to the orthotropic properties that are associated with the longitudinal orientation of a columnar grain. This macroscopic orientation corresponds to a <1 0 0> crystallographic direction. This hypothesis relies on crystallographic analyses by EBSD and by X-diffractometry on the welds [12]. Depending on the metal solidification very different grains structures are produced. Resulting material is anisotropic but furthermore heterogeneous. It is especially true in the case of multipass welding. The elastic constants alter along the wave propagation direction. This leads to a change in phase velocity through Equation (2). Beam deviation, distorsion and even division are then observed [13].

**Results:** In the first part the presentation of existing models of the grains structure is made. In a second part the new model MINA is described and modelling parameters are defined. The MINA model calculates the entire grains structure in a multipass weld. In a third part a comparison of all models is made through simulations of wave propagation.

Several models of grains structures were proposed. Most often their description of the grains structure are simplified and symmetrical whereas most real structures are non symmetrical. In figure 1 are presented several resulting grains structures. Ogilvy proposed a propagation code called RAYTRAIM that calculates the central ray in a grains structure described by mathematical functions. The equation (3) and (4) calculates the angles θ between the direction of grains and axis Oy (figure 1a) [14]. These two equations allow to take into account various geometries of the chamfer. The parameter η varies between 0 and 1, and represents the speed of the grains orientation evolution from the edge towards the centre of the weld.

$$\tan\theta_1 = \frac{T_1(D_1 + z\tan\alpha_1)}{y^{\eta}} \text{ for } y>0 \qquad (3)$$

$$\tan\theta_2 = \frac{T_2|D_2 + z\tan\alpha_2|}{|y^{\eta}|} \text{ for } y>0 \qquad (4)$$

A schematic diagram of the resulting grains structure is presented in figure 1b. Halkjaer and al used Ogilvy's grains structure and consider that locally the material is a transverse isotropic medium [15]. Langerberg and al. also simulated simplified symmetrical structures : grains aligned with the vertical axis or inclined with an angle of 45° (fig. 1c.) [16]. Schmitz and al. used the ray tracing code 3D-Ray-SAFT to calculate the ultrasonic wave propagation. Their empirical symmetrical grains structures are expressed in the form of orientation vectors N with three coordinates. The corresponding N vectors have the following coordinates: $Nx=x^{0.1}$ , Ny = 0, Nz = -0.1z as the transverse plane of the weld corresponds to the plane xz with z the vertical axis [17]. The grains start perpendicular to the weld boundaries and end vertically on the weld central axis. Spies simulated the heterogeneity by splitting up the weld into several layers of transverse isotropic material (fig. 1d) [18]. When the grains structure becomes non-symmetrical a solution proposed by Silk is to define various homogeneous domains (figure 1e and figure 1f) [19].

Several authors made comparison with experimental results. All these qualitative comparisons proved some good agreements. It should be noted that corresponding welds did not always reach the complexity of a heterogeneous structure resulting from manual arc welding.

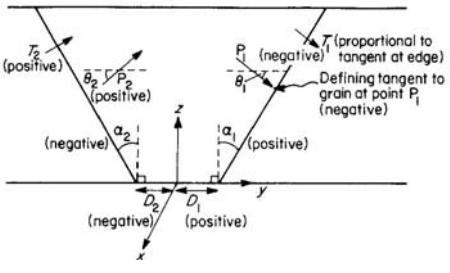


(a)

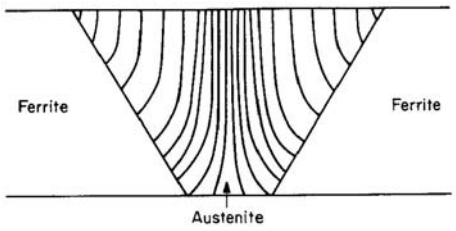


(b)

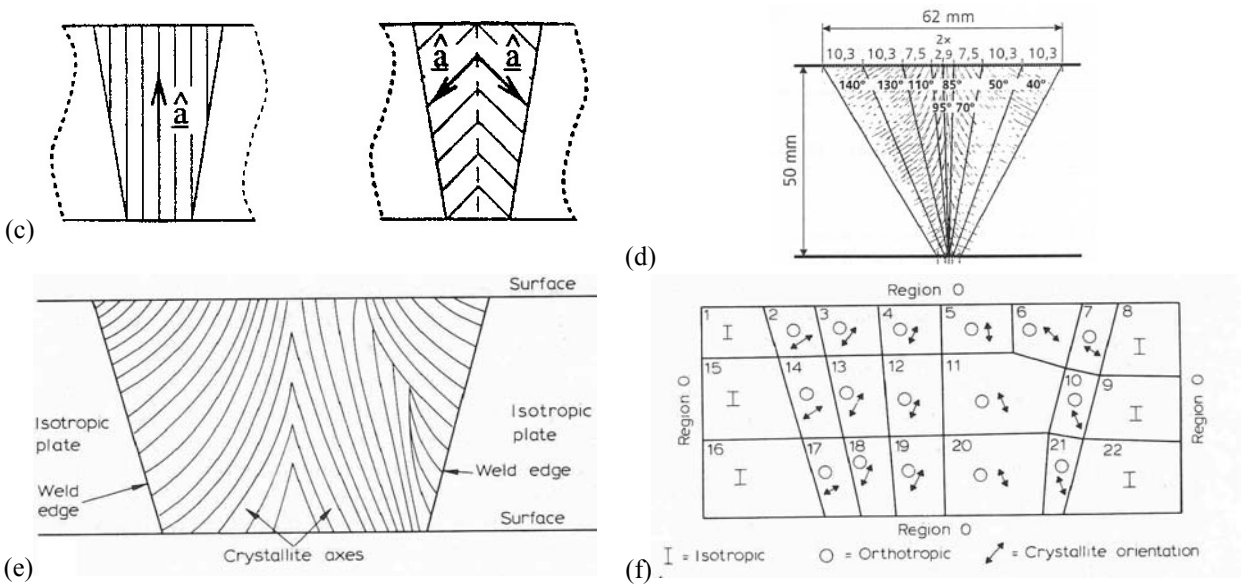


Figure 1. Grains modelling : (a) and (b) used by Ogilvy, (c) used by Langenberg, (d) by Spies (e) and (f) by Silk.

A more precise description of the material is introduced more recently by Chassignole. He defined a 2x2mm mesh to describe the heterogeneous material. The grains orientations had been measured from automatic image analysis of macrographs. He used a two-dimensional finite element code ULTSON allowing the visualization of the complete ultrasonic beam [13, 20]. He also proposed a simplified description that gathered meshes of similar orientations in large domains. Good comparisons are made between simulated and experimental results. It was chosen to keep this scale of modelling for the current work. The aim of the study is to bring more precise comparisons and simulations for the very complex heterogeneous structure obtained in the case of manual multipass welding process. We use the finite element code ATHENA, solving elastodynamic equations, developed by EDF (Electricité de France) and INRIA (national research institute in computer science and automated systems) [21-22]. The transducer central frequency is 2.25 MHz so for the presented results the mesh size is 0.25 mm, about twelve times lower than the wavelength.

Numerous predictive models of grains structure were developed because of the diversity of welding operations (beam of electrons, laser, plasma, TIG, covered electrode) and of alloys that were used (titanium, steel, aluminium). These models have regularly progressed since the sixties when only the temperature gradient was considered. Substantial progress was made in the last decade concerning the understanding of the solidification mechanisms and their modelling [23]. The models are, most of the time, two-dimensional and differ as to the laws that govern the initiation of crystalline growth, the evolution of the solidification front, and the consideration of the grain crystallographic orientation. All these models essentially deal with the automatic or semi-automatic processes and cannot be applied, in their actual form, for manual multipass welding as they required very precise data on the heat source, on the metal composition.

A phenomenological model was developed for welds made with a covered electrode. The model uses information contained in the welding notebook. This model was called **MINA** for **M**odeling an**I**sotropy from **N**otebook of **A**rc welding [10]. The parameters of the welding procedure are as follows: the diameter of the electrodes is imposed and varies according to the passes, the number and the order of passes is up to the operator but must be written, the intensity is imposed according to the diameter of the electrode. The temperature between passes is imposed (<175°C), the initial temperature of the part is also imposed (>5°C). The parameters used in the modelling will be the number and the order of passes and the diameter of the electrodes. A proportionality rule is defined to calculate the pass thickness from the electrode diameter.

The phenomenological model is composed of four steps: the description of the temperature gradient directions in the weld pool, the description of the remelting of passes, the description of the incline of passes and the description of the grains growth. The weld pool geometry is modelled by two parabolic curves centred on O and

C points (figure 2). From this weld pool representation, it is simple to express the direction of the local temperature gradient geometrically from the centre of symmetry D. The gradient angle from the vertical axis is denoted by $\alpha_g$. When a new pass is deposited, be it laterally or vertically in relation to the previous pass, this creates partial remelting. **$R_L$ parameter is the lateral remelting rate and $R_V$ is the vertical remelting rate**. These two parameters, $R_L$ and $R_V$, are the most important ones and are obtained by analysis of macrographs of several similar welds.

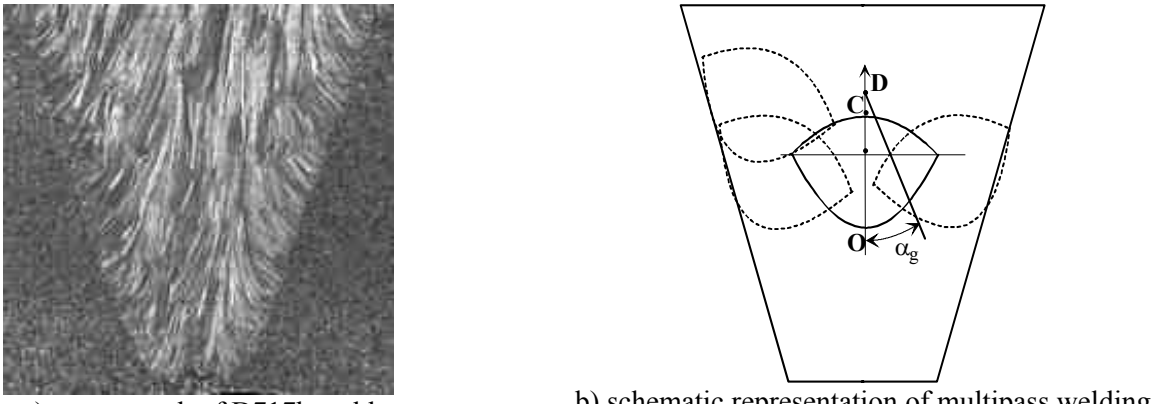


a) macrograph of D717b weld b) schematic representation of multipass welding

Figure 2. Macrograph of a V-weld and its schematic representation.

However even in this simple case, the operator makes his choice in relation to the geometry of the welded joint for the order in which he deposits the passes, which obliges him to tilt the electrode; this causes an incline of the welding pool. The hypothesis is that this phenomenon can be described simply by a rotation of the direction of the temperature gradient without changing the geometric shape of the pass. The analysis of the welding technique and the macrographs observations lead to distinguish two cases. When a pass is deposited and leans on a previous pass, the temperature gradient is inclined by an angle denoted $\theta_C$ lower than the observed angle, noted $\theta_B$, when a pass leans on the sidewall. This second angle reproduces the influence of the weld geometric shape. When a pass is deposited and it leans to its left or right, the simulated temperature gradient is symmetric with respect to the vertical line ($\theta_C = 0$). The model MINA automatically calculates these **two parameters $\theta_B$ and $\theta_C$** depending on the pass location written in the welding notebook.

Grains growth is governed by three physical phenomena: the epitaxial growth, the influence of the temperature gradient, and the selective growth, which is the result of the competition between the grains. If the heating conditions do not cause recrystallisation in the previous pass, there is epitaxial growth when the metal in the fusion of a new pass solidifies so that the grains take the crystalline orientation of the pass that is just below. Grains tend to follow the direction of the local temperature gradient, i.e. perpendicular to the isotherms. Grains with a <1 0 0> direction parallel to the heat flow direction grow fastest and hence stifle the growth of unsuitably oriented grains. Grains whose orientations are quite close to the heat flow direction turn towards the direction of the temperature gradient by growth of secondary arms. The grains can thus make small turns to follow the direction of the gradient and do so by epitaxy. From these three physical phenomena the MINA model calculates the final grain angle noted $\alpha_n$. To take into account the fact that a grain slowly grows from its initial direction towards the direction of the temperature gradient $\alpha_g$, and also to take into account the selective growth, an iterative formulation is introduced which allows representing the influence of the gradient orientation on a variable scale. Formulae can be applied **n** times in a mesh to simulate possible changes in grain direction at a smaller scale. This model was validated by macrographs analysis on a set of welds done with the same welding notebook by two different welders [10].

A simple case was chosen to compare with other models. The austenitic steel weld is symmetrical, has a 36 mm height and was obtained with twenty seven passes. All of them are executed from the left to the right. MINA parameters are $R_L = 0.47$; $R_V = 0.26$; $\theta_B = 18°$, $\theta_C = 12°$, n = 10. In figure 2a is shown a macrograph of the weld (noted D717b) where the grains directions are clearly seen. The global grains structure is non-symmetrical due to

the remelting process and the incline of the electrode. Real grains orientations were measured and represented in a square mesh corresponding to the chosen scale of 2x2 mm (figure 3a). The calculated grains orientations with the MINA model are represented in figure 3b.

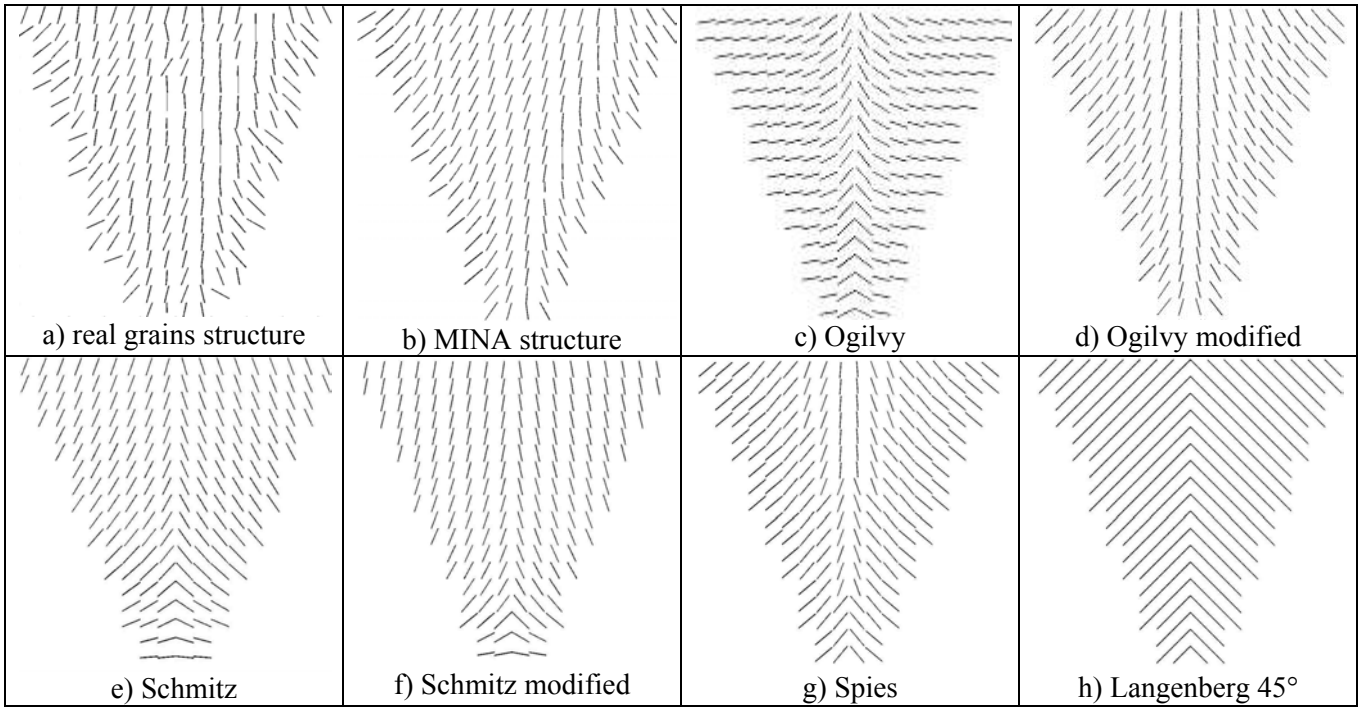


Figure 3. Resulting grains structure for several modelling techniques

Ogilvy's model was used with author's parameters in a symmetrical configuration: T = 0.3 and η= 0.85 (figure 3c). Clearly the resulting grains orientations are not close enough to the real ones. Parameters have to be adjusted to the weld geometry. A better modelling is obtained with T=2 and η=0.9. Increasing T makes grains more vertical and, as indicated by Ogilvy, η parameter should be close to one. If this parameter is too low variations along horizontal axis are inexistent. Equations proposed by Schmitz were used for creating a grains structure (figure 3e) with grains too much aligned along horizontal axis in the bottom of the weld. Increasing the ratio between Nz and Nx by a factor two produces a more realistic structure (figure f) but it produces also too much grains aligned vertical axis. As parameters Nz and Nx are not correlated it is not possible to obtain good orientations everywhere in the weld. An equation with two spatial variables, as for Ogilvy's model, would be better. Spies's decomposition in homogeneous domains is used after a scale correction to adapt the dimensions of the domains to the size of D717b weld (figure 3h). A representation of the Langenberg's proposition corresponding to the 45° directions is shown in the last part of the figure 3.

These grains structures are used to produce corresponding material descriptions for the ATHENA code. Inspection simulations are made with a contact transducer at normal incidence for the clarity of the comparison. The probe diameter is 0.5". ATHENA code generates a visualisation of the ultrasonic beam (darker color in the following figures). Results are represented in figure 4 with the transducer positioned 8 mm left from the middle of the weld outer surface. It is one of the positions where the beam is splitting for the D717b weld.

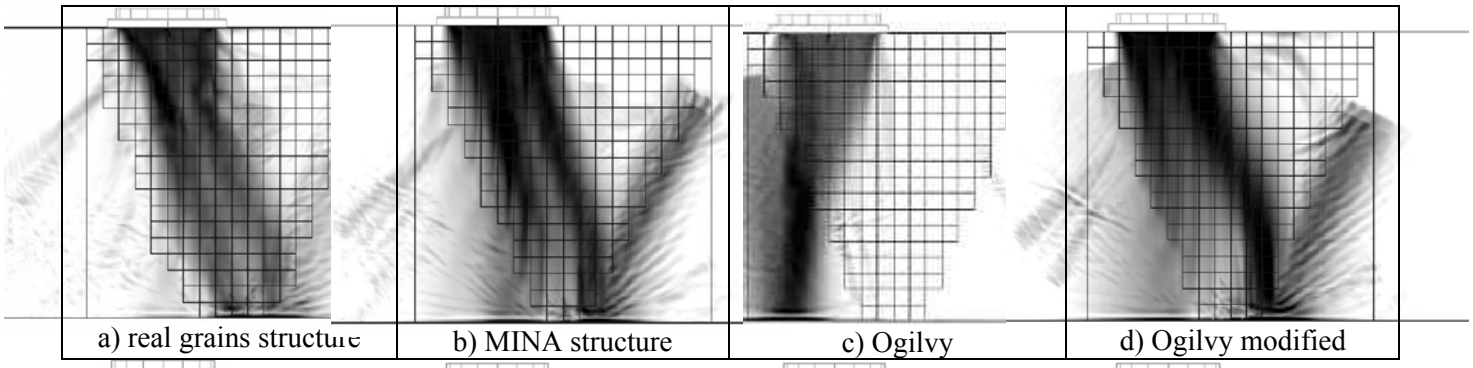

a) real grains structure b) MINA structure c) Ogilvy d) Ogilvy modified

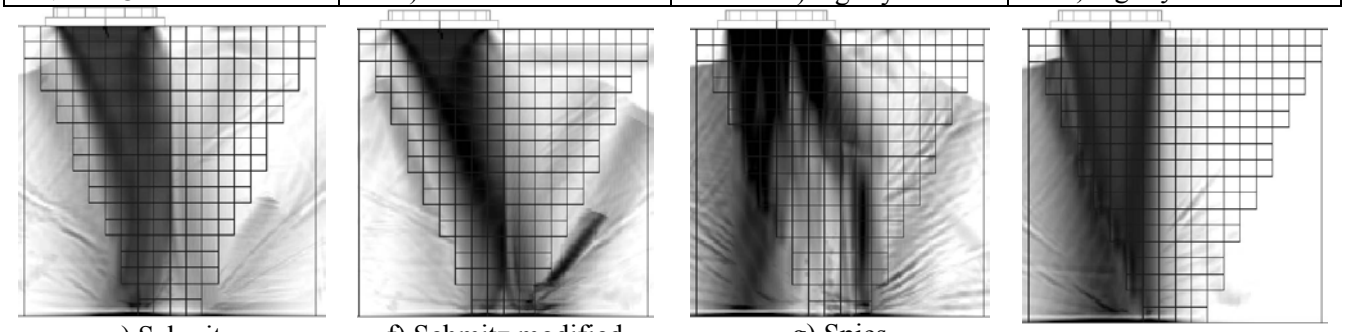

e) Schmitz f) Schmitz modified g) Spies d) Langenberg 45°

Figure 4. Resulting ultrasonic wave propagation simulated with ATHENA code in simulated grains structure.

More quantitative comparisons are made with the echodynamic curve at the bottom of the weld. This curve represents the distribution, along the horizontal axis, of the maximum of amplitude of the wave reaching the bottom of the weld. Two probe positions were used: in the first one the transducer was in the middle of the weld outer surface, in the second one the transducer was 8 mm left from the middle of the weld (figure 5). For each position we classify the modelling in two groups: lower and better results. The classification was made regarding the number of peaks and their thicknesses. The number and the positions of the peaks of this curve are good indicators of beam deviation and the beam splitting. Their study allows validating the grains structure modelling techniques.

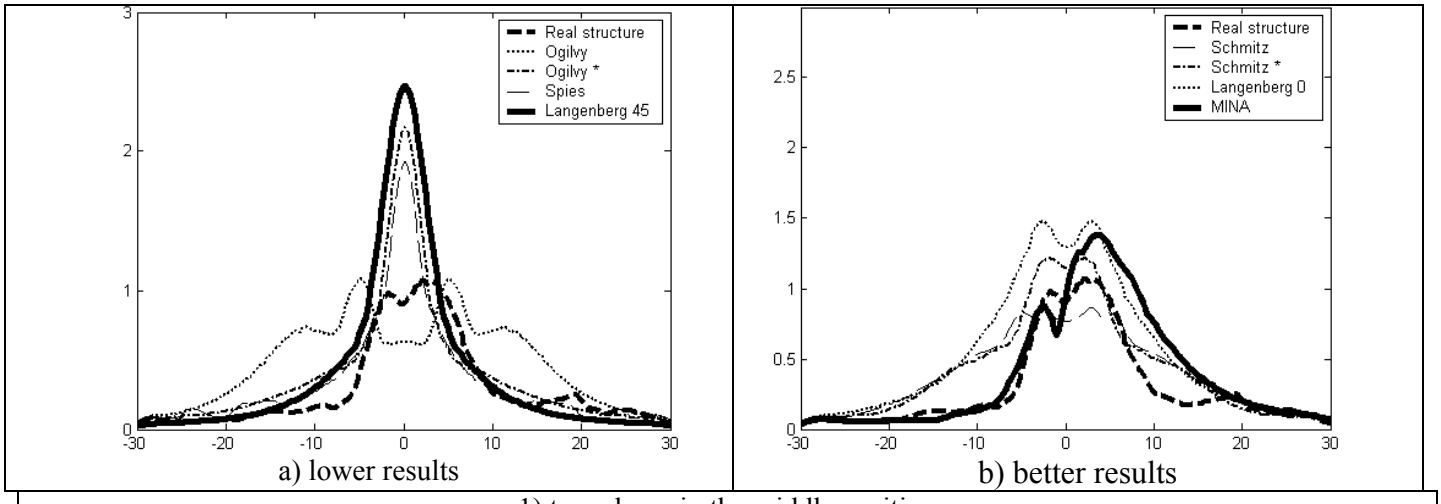


a) lower results b) better results

1) transducer in the middle position

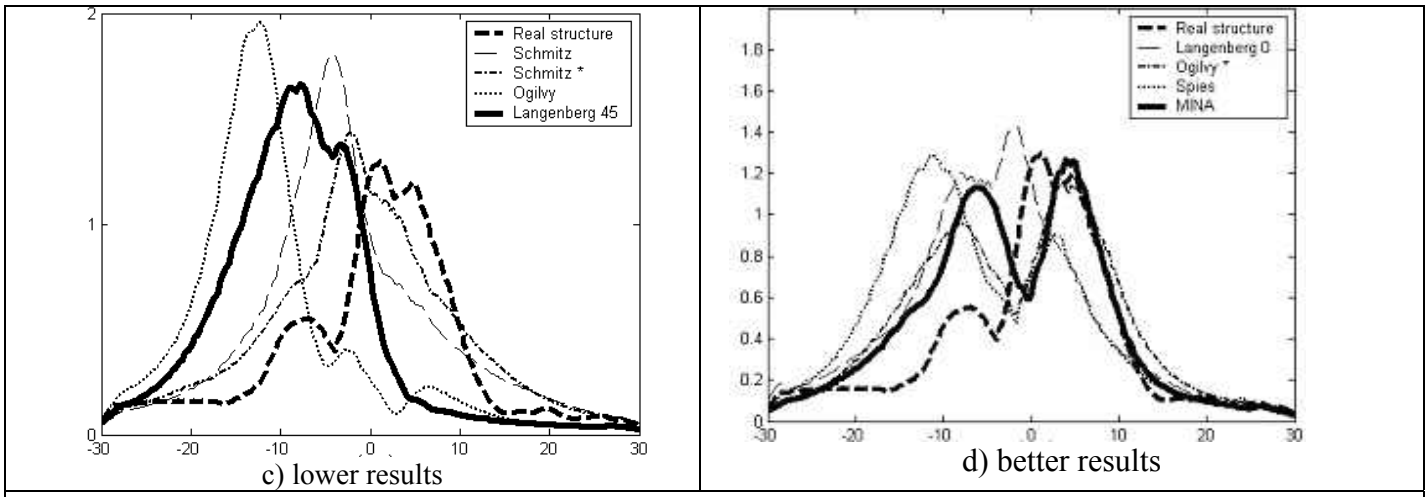


c) lower results

d) better results

2) transducer at 8 mm left from the middle of the weld outer surface

Figure 5. Resulting echodynamic curves (arbitrary units for amplitude scale, mm for the horizontal axis)

**Discussion:** The beam is splitting in the real structure and this effect is correctly reproduced in the grains structure calculated with the model MINA. Few modelling techniques reproduce this splitting (figure 4). After the adaptation of the modelling parameters to obtain a grains structure close to the real one, Ogilvy's modelling techniques replicate this effect. We can note that the decomposition in homogeneous domains according to Spies' proposition creates an overestimated splitting effect without modification of the initial grains orientations.

When the transducer is in the middle position several models reduce the reality of the beam divergence, the resulting amplitude is then greater on the echodynamic curve (figure 5a). When the transducer is positioned on the left several models overestimated the beam deviation and do not simulate the beam splitting (figure 5c). MINA produces the best results. No others models give good results in the two positions. The grains structure completely vertically oriented gives curiously not too far results from the real ones in the these positions.

The MINA results are very encouraging as it was shown there is good repeatability of the grain structure along the welding direction, so a 2D-growth model can be used in the transverse plane. The 2D growth represents an accurate approximation, even though it is true that some grains leave the transverse plane [14][20].

**Conclusions:** The new model MINA has been proven to be very efficient and superior to previous modelling techniques despite a simple configuration in the case of multipass welding. The austenitic steel weld D717b was obtained with twenty seven passes; all of them are executed from the left to the right. In numerous industrial cases the order of passes varies from one layer to another layer. A more asymmetrical grains structure is then obtained. MINA modelling technique brings a great advance by taking into account the order of passes. For different order of passes the other models calculate only one grains structure as they are mainly founded on the chamfer geometry. The manual adaptation of model parameters (Ogilvy, Schmitz) demonstrates the interest of developing inverse methods to calculate optimal parameters when very precise modelling is required. Another method was developed to compare grains orientations using contour maps of differences between modelling and measured orientations [10]. The final validation will be made with experimental results in oblique incidence. This work is in progress. Another perspective concerns the modelling of 3D structures for vertical or overhead positions of welding.

## References:

[1] M. Spies, Modeling of transducer fields in weld material : a comparison of three generically different approaches, Review of progress in Quantitative Nondestructive Evaluation, Plenum Press, 2000, **19** : 961-968

[2] N. Gengembre, Modélisation du champ ultrasonore rayonné dans un solide anisotrope et hétérogène par un traducteur immergé, Thèse Université Paris 7, 1999, 143p (in french)

[3] N. Gengembre, A. Lhemery, Pencil method in elastodynamics : application to ultrasonic field computation, Ultrasonics, 2000, **38** : 495-499

[4] M.G. Silk, A.M. Stoneham, J.A.G. Temple, The reliability of non-destructive inspection. Assessing the assessment of structures under stress, Bristol, Adam Hilger, 1987

[5] R.W. Nichols, A review of the work related to defining the reliability of non-destructive testing, Nuclear Engineering and Design, 1989, **114** : 1-32
[6] P. Lemaitre, T.D. Koble, S.R. Doctor, Summary of the PISC round robin results on wrought and cast austenitic steel welments, part I: wrought-to-wrought capability study, International Journal of Pressure Vessels and Piping, 1996, **69** : 5-19
[7] P. Lemaitre, T.D. Koble, S.R. Doctor, Summary of the PISC round robin results on wrought and cast austenitic steel welments, part II: wrought-to-cast capability study, International Journal of Pressure Vessels and Piping, 1996, **69** : 21-32.
[8] P. Lemaitre, T.D. Koble, S.R. Doctor, Summary of the PISC round robin results on wrought and cast austenitic steel welments, part III: cast-to-cast capability study, International Journal of Pressure Vessels and Piping, 1996, **69** : 33-44.
[9] D. Royer, E. Dieulesaint, Elastic waves in solids I, Free and Guided Propagation, Springer Verlag, 1999, 374p
[10] J. Moysan, A. Apfel, G. Corneloup, B. Chassignole, Modelling the grain orientation of austenitic stainless steel multipass welds to improve ultrasonic assessment of structural integrity, International Journal of Pressure Vessels and Piping, 2003, **80** : 77-85.
[11] B. Castagnede, J.T. Jenkins, W. Sachse, Optimal determination of the elastic constants of composite materials from utrasonic wavespeed measurements, J. Appl. Phys., 1990, **67** : 2753-2761
[12] D. Ducret, R. El Guerjouma, P. Guy, M. R'Mili, J.C. Baboux, Merle P., Characterisation of anisotropic elastic constants of continuous alumina fibre reinforced aluminium matrix composite processed by medium pressure infiltration, Composites : Part A., 2000, **31** : 45-55
[13] B. Chassignole, D. Villard, M. Dubuget, J.C. Baboux, R. El Guerjouma, Characterization of austenitic stainless steel welds for ultrasonic NDT, Rewiew of Progress in Q.N.D.E., 2000, **20** : 1325-1332
[14] J.A. Ogilvy, Computerized ultrasonic ray tracing in austenitic steel, NDT&E International, 1985, **18** : 67-77
[15] S. Halkjaer, M.P. Sorensen, W.D. Kristensen, The propagation of ultrasound in a austenitic weld, Ultrasonics, 2000, **38** : 256-261
[16] K.J. Langenberg, R. Hannemann, T. Kaczorowski, R. Marklein, B. Koehler, C. Schurig, F. Walte, Application of modeling techniques for ultrasonic austenitic weld inspection, NDT&E International, 2000, **33** : 465-480.
[17] V. Schmitz, F. Walte, S.V. Chakhlov, 3D ray tracing in austenite materials, NDT&E International, 1999, **32** : 201-213.
[18] M. Spies, M. Kroning, Ultrasonic inspection of inhomogeneous welds simulated by a gaussian beam superposition, Review of progress in Quantitative Nondestructive Evaluation, Vol. 18, Plenum Press, 1999, p 1107-1113
[19] M.G. Silk, A computer model for ultrasonic propagation in complex orthotropic structures, Ultrasonics,1981 , **19** : 208-212.
[20] B. Chassignole, Influence of the metallurgical structure of austenitic stainless steel welds on the ultrasonic non destructive testing, PhD Thesis, ISAL 0107, INSA Lyon (2000) 207 p. (french).
[21] E. Becache, P. Joly, C. Tsogka, An analysis of new mixed finite elements for the approximation of wave propagation problems, SIAM J Numer Anal, 2000, **37** : 1053-84.
[22] E. Becache, P. Joly, C. Tsogka, Application of the fictitious domain method to 2D linear elastodynamic problems, J. Comput Acoust., 2001, **9** :1175-202.
[23] W.J. Boettiner, S.R. Coriell, A.L. Greer, A. Karma, W. Kurz, M. Rappaz, R. Trivedi, Acta Mater., 2000, **48 :** 43-70